

# Correction of Permeability with Pore Radius of Tight Junctions in Caco-2 Monolayers Improves the Prediction of the Dose Fraction of Hydrophilic Drugs Absorbed by Humans

Ryoichi Saitoh,<sup>1,2</sup> Kiyohiko Sugano,<sup>1</sup>  
Noriyuki Takata,<sup>1</sup> Tatsuhiko Tachibana,<sup>1</sup>  
Atsuko Higashida,<sup>1</sup> Yoshiaki Nabuchi,<sup>1</sup> and  
Yoshinori Aso<sup>1</sup>

Received December 16, 2003; accepted January 29, 2004

**Purpose.** To improve predictions of fraction dose absorbed (Fa) for hydrophilic drugs, a correction of paracellular permeability using the pore radius of tight junctions (TJs) in Caco-2 monolayers was performed.

**Methods.** The apparent permeability coefficient ( $P_{app}$ ) of drugs was measured using the Caco-2 assay and the parallel artificial membrane permeation assay (PAMPA), and values were corrected with the pore radius of TJs.

**Results.** An equation for calculating the pore radius of TJs from the  $P_{app}$  of lucifer yellow was obtained. The optimal pore radius of TJs in Caco-2 monolayers for predicting human Fa was calculated to be 7 Å. The correlation between the actual and predicted Fa was improved by using the  $P_{app}$  corrected with the pore radius of TJs. Permeability in the PAMPA, which was corrected using the pore radius and membrane potential, was well correlated with that in the Caco-2 assay. Most of the hydrophilic drugs tested in this study were absorbed mainly through the paracellular pathway.

**Conclusions.** The results suggest the necessity of optimizing paracellular permeation for the prediction of Fa, and also the importance of the paracellular pathway to the absorption of hydrophilic drugs. This method might contribute to the setting of appropriate dosages and the development of hydrophilic drugs.

**KEY WORDS:** artificial membrane; Caco-2 monolayer; hydrophilic drug; paracellular permeation; prediction.

## INTRODUCTION

Because the low bioavailability of drugs is a major cause of interindividual variability, it is difficult to prescribe such drugs properly. Intestinal absorption is one of the principal determinants of the bioavailability of orally administered drugs. Therefore, it is important to implement membrane penetration screening of newly synthesized compounds and to identify those compounds with excellent membrane permeation in drug development (1).

There are two routes of transepithelial drug transport by passive diffusion: the transcellular route through the cell membrane and the paracellular route from the tight junction (TJ) to the lateral space. Lipophilicity is a key factor in drug absorption (2), and in hydrophilic drugs, the contribution of

the transcellular route is thought to be small. Therefore, it has been considered that the fraction dose absorbed (Fa) in humans for hydrophilic drugs is low.

However, hydrophilic drugs with high Fa value exist. Metformin, a biguanide antihyperglycemic agent for the treatment of diabetes, was reported to have high Fa value (86%) in humans (3). Moreover, the bioavailability of polyethylene glycol was increased by reducing its molecular weight (4). These reports suggested the importance of the paracellular pathway in the absorption of hydrophilic drugs. However, the contribution of paracellular pathway in humans has not been discussed yet. Therefore, in order to comprehend the mechanism by which hydrophilic drugs are absorbed, it is important to quantify the contribution of each absorption pathway.

The Caco-2 cell line, which is derived from colon adenocarcinoma, undergoes spontaneous differentiation in culture, forming monolayers of polarized enterocytes that exhibit morphological and functional similarities to small intestinal epithelial cells (5). Although the permeation assay using Caco-2 monolayers is a standard method for determining the apparent permeability coefficient ( $P_{app}$ ) and predicting human Fa value of drug candidates in drug development, the  $P_{app}$  of Caco-2 monolayers and subsequently the predicted human Fa value is affected by experimental conditions, such as passage number, cultivation period, and pH of the transport medium (6,7). Variations in permeation via the paracellular pathway have been thought to be one of the causes of the variability in the  $P_{app}$  of Caco-2 monolayers. The pore radius of TJs has a major influence on drug permeation through the paracellular pathway (8). For this reason, in order to predict human Fa accurately, it is necessary to optimize the pore radius of TJs in Caco-2 cells. However, it is not easy to maintain a uniform pore radius of TJs. Therefore, it is preferable to correct the  $P_{app}$  using the pore radius of TJs measured in each monolayer.

In the current study, an advanced method to measure the pore radius of TJs was established. By correcting the pore radius, the interexperimental variability in the  $P_{app}$  values of hydrophilic drugs was markedly improved. Also, the optimal pore radius of TJs for predicting Fa in humans using the  $P_{app}$  for Caco-2 monolayers was assessed. Furthermore, the contribution of the absorption pathway was estimated by comparing the Caco-2 assay with the parallel artificial membrane permeation assay (PAMPA).

## MATERIALS AND METHODS

### Chemicals

[<sup>14</sup>C]mannitol (59 mCi/mmol) and [<sup>14</sup>C]urea (55 mCi/mmol) were purchased from Amersham Pharmacia Biotech (Buckinghamshire, UK) and Moravex Biochemicals (Brea, CA, USA), respectively. Ketoprofen, imipramine, zidovudine, doxycycline, hydrocortisone, prazosine, metformin, tetracycline, guanabenz, furosemide, metaproterenol, famotidine, bromocriptine, cefuroxime, cefazolin, ceftriaxone, and lucifer yellow were purchased from Sigma Chemical (St. Louis, MO, USA). Verapamil and antipyrine were obtained from Wako Pure Chemicals (Osaka, Japan). Cymarin was purchased from Aldrich Chemical Company (Milwaukee, WI, USA). Chlorothiazide was bought from Alexis corporation

<sup>1</sup> Fuji Gotemba Research Laboratories, Chugai Pharmaceutical Co., Ltd., Gotemba, Shizuoka 412-8513, Japan.

<sup>2</sup> To whom correspondence should be addressed. (e-mail: saitorui@chugai-pharm.co.jp)

(San Diego, CA, USA). L- $\alpha$ -phosphatidylserine (PS), L- $\alpha$ -phosphatidylinositol (PI), and cholesterol (CHO) were obtained from Sigma Chemical. L- $\alpha$ -phosphatidylcholine (PC) and L- $\alpha$ -phosphatidylethanolamine (PE) were provided by Nippon Oil & Fats Corporation (Tokyo, Japan). 1,7-Octadien was purchased from Tokyo Kasei Kogyo (Tokyo, Japan). All other reagents used were of analytical grade.

### Preparation of Caco-2 Monolayers

The Caco-2 cell line was obtained from American Type Culture Collection (Rockville, MD, USA) at passage 17. The cells were cultured in Dulbecco's Modified Eagle's Medium (DMEM) supplemented with 10% fetal bovine serum (FBS), 1% nonessential amino acids (NEAA), and 2 mM L-glutamine in a humidified incubator (5% CO<sub>2</sub>, 37°C). The Caco-2 monolayer was prepared using the Biocoat HTS Caco-2 Assay System (Becton Dickinson Bioscience, Bedford, MA, USA) with some modifications. Briefly, before reaching full confluency, the cells were detached with 0.25% trypsin and 0.02% EDTA and removed from the culture flask. On day 0, the cells were plated at a density of  $1.29 \times 10^5$  cells/cm<sup>2</sup> in DMEM supplemented with 0.5% FBS, 1% NEAA, and 2 mM L-glutamine on fibrillar collagen-coated inserts (1.0  $\mu$ m pore, 0.31 cm<sup>2</sup> growth area). On day 3, the medium was replaced with Basal Seeding Medium containing MITO+ Serum Extender (BSM). On day 5, the BSM was replaced with Enteo-STIM Differentiation Medium containing MITO+ Serum Extender. Transport experiments were performed on day 7.

### Permeation Experiments in Caco-2 Monolayers

The transport of each drug in the apical to basal direction was examined under a pH gradient (apical pH = 6.0, basal pH = 7.4). Hank's balanced salt solution (HBSS) containing 25 mM glucose and 1% DMSO was used. Prior to the experiments, the monolayer was washed twice with HBSS. Transport experiments were initiated by adding HBSS (pH 6.0) containing a drug listed in Table I or the radiolabeled marker compound to the apical side of the monolayer. Lucifer yellow (0.5 mg/ml) was used as a paracellular marker compound to check the integrity of the monolayer during the incubation. The monolayer was incubated for up to 2 h at 37°C.

The radioactivity of urea and mannitol in the basal compartment was counted using a TRI-CARB liquid scintillation counter (PerkinElmer, Shelton, CT, USA). The concentration of the following drugs, verapamil, ketoprofen, imipramine, zidovudine, antipyrine, doxycycline, hydrocortisone, prazosin, and guanabenz, in the apical and basal compartments was determined by LC/MS (micromass ZQ-alliance 2790 separation module, Waters, MA, USA) with a C18 column (Xterra MS-C18 3.5  $\mu$ m 2.1  $\times$  30 mm, Waters). The eluents consisted of 2 mM ammonium acetate:acetonitrile (MeCN):ammonia in ratios of 100:0:0.002 (v/v, solvent A) and 10:90:0.002 (v/v, solvent B). Elution was accomplished using a linear gradient that consisted of ramping from 3% to 100% B during 2.5 min. The concentration of furosemide, metaprotenol, chlorothiazide, cefroxime, cefazolin, tetracycline, ceftriaxone, and famotidine was quantified by HPLC (LC-10A, Shimadzu, Kyoto, Japan) with a C18 column (Mightysil RP-18 GP 3  $\mu$ m 4.6  $\times$  100 mm, Kanto Kagaku, Tokyo, Japan).

**Table I.** P<sub>app</sub> Determined from Caco-2 Monolayer and Parallel Artificial Membrane Permeation Assay

Compound	MW	PrologD pH 6.0*	Fa%†	P <sub>caco-2</sub> ( $\times 10^{-6}$ cm/s)‡	P <sub>am</sub> ( $\times 10^{-6}$ cm/s)§
Ketoprofen	254.3	1.18	100	88.0 $\pm$ 1.2 (1.36)	33.8 $\pm$ 2.1
Imipramine	280.4	1.17	100	8.49 $\pm$ 1.28 (15.1)	42.1 $\pm$ 0.2
Verapamil	454.6	3.25	100	3.95 $\pm$ 1.10 (27.8)	38.4 $\pm$ 0.9
Zidovudine	267.2	0.06	100	13.4 $\pm$ 1.7 (12.7)	3.65 $\pm$ 0.73
Antipyrine	188.2	1.79	97	45.3 $\pm$ 2.1 (4.64)	9.12 $\pm$ 0.70
Doxycycline	444.4	-2.21	95	17.5 $\pm$ 0.3 (1.71)	27.8 $\pm$ 0.3
Hydrocortisone	362.5	1.27	91	21.8 $\pm$ 3.1 (14.2)	18.8 $\pm$ 0.6
Prazosin	383.4	1.31	86	2.27 $\pm$ 0.51 (22.5)	18.2 $\pm$ 1.1
Metformin	129.2	-6.13	86	1.09 $\pm$ 0.62 (56.9)	<0.27
Tetracycline	444.4	-2.06	78	1.62 $\pm$ 0.90 (55.6)	4.70 $\pm$ 0.16
Guanabenz	231.1	-0.68	75	8.37 $\pm$ 0.45 (5.38)	8.52 $\pm$ 0.66
Furosemide	330.7	0.25	61	1.76 $\pm$ 0.21 (11.9)	3.60 $\pm$ 0.08
Cymarin	548.7	1.53	47	3.30 $\pm$ 1.02 (30.9)	4.13 $\pm$ 1.34
Metaprotenol	211.3	-1.65	44	0.67 $\pm$ 0.64 (95.5)	<0.27
Famotidine	339.5	-4.55	38	1.20 $\pm$ 0.07 (5.83)	<0.05
Bromocriptine	654.6	3.60	28	2.11 $\pm$ 1.19 (56.4)	0.99 $\pm$ 0.17
Chlorothiazide	295.7	-2.08	13	0.92 $\pm$ 0.23 (25.0)	0.31 $\pm$ 0.20
Cefazolin	454.5	-5.22	6¶	1.03 $\pm$ 0.21 (20.4)	0.05 $\pm$ 0.01
Cefuroxime	424.4	-3.29	5	0.61 $\pm$ 0.43 (70.5)	0.07 $\pm$ 0.01
Ceftriaxone	554.6	-4.68	1	1.13 $\pm$ 1.39 (123)	0.03 $\pm$ 0.02

\* PrologD values were calculated using PALLAS (ver 3.0, CompuDrug).

† Fa values in humans were cited from Ref. 3.

‡ Data are represented as the mean  $\pm$  SD for 3 to 11 experiments. CV(%) values are in parentheses.

§ Artificial membrane permeability coefficient measured with the PC (0.8%)/PE (0.8%)/PS (0.2%)/PI (0.2%)/CHO (1.0%)/1,7-octadien membrane at pH 6.0. Data are represented as the mean  $\pm$  SD in triplicate.

¶ The Fa value for cefazolin was estimated as the percentage of the cumulative excreted amount in urine after oral and intravenous administration (18,19).

The eluents were H<sub>2</sub>O:MeCN:trifluoroacetic acid (TFA) in ratios of 100:0:0.1 (v/v, solvent A) and 20:80:0.1 (v/v, solvent B). Gradient elution was performed using an increase of 3% to 60% B during 10 min. The UV detector was set to 280 nm except for ceftriaxone (250 nm) and tetracycline (360 nm). The concentration was determined by HPLC using a Mightysil C18 column for bromocriptine and cymarin, and using a CAPCELLPACK C18 column (3 μm 4.6 × 150 mm, Shiseido, Tokyo, Japan) for metformin. The eluent for bromocriptine consisted of tetraethylamine (pH 3.0):H<sub>2</sub>O:MeCN (0.2:70:30 (v/v)). The eluent for cymarin was H<sub>2</sub>O:MeCN:TFA at 66:34:0.1 (v/v). The eluent for metformin was 5 mM PIC B7 reagent (Waters)-MeOH (80:20 (v/v)). The fluorescence detector for detecting bromocriptine was set to excitation and emission wavelengths of 330 nm and 405 nm, respectively. A wavelength of 220 nm was used to detect cymarin and metformin. The concentration of LY was determined using the microtiter plate reader Spectramax 190 (Molecular Devices, CA, USA) at excitation and emission wavelengths of 430 nm and 535 nm, respectively.

The apparent permeability coefficient (P<sub>app</sub>) of each drug was calculated with the equation 1;

$$P_{app} = \frac{dQ}{dt} \times \frac{1}{A \times C_0} \quad (1)$$

where dQ/dt is the flux of a drug across the monolayer (μmol/s), A is the surface area of the monolayer (cm<sup>2</sup>), and C<sub>0</sub> is the initial drug concentration on the apical side (mM).

### Calculation of Pore Radius of TJs in Caco-2 Monolayers

On the basis of the general phenomenon of molecular size-restricted diffusion within a negative electrostatic field of force, the permeability coefficients of cationic (P<sup>+</sup>), anionic (P<sup>-</sup>) and neutral (P<sup>0</sup>) ions are

$$P^+ = \frac{\varepsilon D}{\delta} F \left( \frac{r}{R} \right) \left( \frac{\kappa}{1 - e^{-\kappa}} \right) \quad (2)$$

$$P^- = \frac{\varepsilon D}{\delta} F \left( \frac{r}{R} \right) \left( \frac{\kappa}{e^{\kappa} - 1} \right) \quad (3)$$

and

$$P^0 = \frac{\varepsilon D}{\delta} F \left( \frac{r}{R} \right) \quad (4)$$

where ε is the porosity, δ is the pore length, and D is the aqueous diffusion coefficient of the molecules (9). The dimensionless electrochemical energy parameter (κ) is expressed in Eq. 5;

$$\kappa = \frac{ez|\Delta\Psi|}{kT} = Cz \quad (5)$$

where e is the unit charge of the ion, z is the absolute value of the valence, kT is the thermal energy, and Δψ is the absolute value of the potential difference across the tight junction. The dimensionless molecular sieving Renkin function for cylindrical channels is

$$F\left(\frac{r}{R}\right) = \left[ 1 - \left(\frac{r}{R}\right) \right]^2 \left[ 1 - 2.104 \left(\frac{r}{R}\right) + 2.09 \left(\frac{r}{R}\right)^3 - 0.95 \left(\frac{r}{R}\right)^5 \right] \quad (6)$$

which compares the molecular radius (r) with the pore radius (R) and where 0 < F(r/R) < 1 (10).

The pore radius of the paracellular route was calculated as follows. P<sub>app</sub> of urea (P<sub>urea</sub>) and mannitol (P<sub>mannitol</sub>) were expressed in equations 7 and 8.

$$P_{urea} = \frac{\varepsilon D_{urea}}{\delta} F \left( \frac{r_{urea}}{R} \right) \quad (7)$$

$$P_{mannitol} = \frac{\varepsilon D_{mannitol}}{\delta} F \left( \frac{r_{mannitol}}{R} \right) \quad (8)$$

Because ε and δ were the same values in each monolayer, the ratio of the P<sub>urea</sub> and P<sub>mannitol</sub> was expressed as Eq. 9.

$$\frac{P_{urea}}{P_{mannitol}} = \frac{D_{urea} \times F \left( \frac{r_{urea}}{R} \right)}{D_{mannitol} \times F \left( \frac{r_{mannitol}}{R} \right)} \quad (9)$$

D is inversely proportional to the molecular radius, so Eq. 9 was converted to Eq. 10. Molecular radii of urea and mannitol used were 2.67 Å and 4.10 Å, respectively (8).

$$\frac{P_{urea}}{P_{mannitol}} = \frac{r_{mannitol} \times F \left( \frac{r_{urea}}{R} \right)}{r_{urea} \times F \left( \frac{r_{mannitol}}{R} \right)} \quad (10)$$

### Permeation Experiments Using an Artificial Membrane

A 96-well plate (acceptor compartment) was filled with a 50 mM sodium phosphate buffer (pH 6.0) containing 5% DMSO. The hydrophobic filter plate (donor compartment) was fixed on the buffer-filled plate. The filter material in each well was wetted with 5 μl of artificial membrane solution, which consisted of PC (0.8%)/PE (0.8%)/PS (0.2%)/PI (0.2%)/CHO (1.0%)/1,7-octadiene (97.0%). The drug solution containing 5% DMSO was added to the filter plate and incubated for 2 or 15 h at 37°C. The concentration of compound in the acceptor compartment was determined by UV spectroscopy, using the Spectramax 190 over a range of 240 to 440 nm at intervals of 10 nm. Artificial membrane permeability (P<sub>am</sub>) was calculated with Eq. 11 (11);

$$P_{am} = -2.303 \times \frac{V_{dn} \times V_{ac}}{V_{dn} + V_{ac}} \times \frac{1}{S \times t} \times \log \left( 1 - \frac{\text{flux}\%}{100} \right) \quad (11)$$

$$\text{flux}\% = \frac{A_{ac}}{A_{ref}} \times 100 \quad (12)$$

where V<sub>dn</sub> is the volume of the donor compartment (0.1 mL), V<sub>ac</sub> is the volume of the acceptor compartment (0.38 mL), A<sub>ac</sub> is the UV absorbance of the solution of the acceptor compartment, A<sub>ref</sub> is the UV absorbance of the reference solution, S is the membrane surface area (0.266 cm<sup>2</sup>), and t is the incubation time (s). 5% DMSO did not affect the P<sub>am</sub> of drugs (11).

### Correction of PAMPA Permeability Using a Paracellular Pathway Prediction Model

Because paracellular permeation of drugs was not evaluated using traditional PAMPA, Sugano *et al.* proposed the

PAMPA-PP-RP model, which combined  $P_{am}$  and the Renkin function (Eq. 6) and could predict the paracellular permeation (3). The permeability coefficient of PAMPA included in the paracellular permeation ( $P_{tot}$ ) value was obtained in Eq. 13:

$$P_{tot} = P_{am} + \frac{B}{A} \times \frac{1}{r} \times F \left( \frac{r}{R} \right) \left[ r^0 + \sum_{z(z \neq 0)} f^z \left( \frac{Cz}{1 - e^{Cz}} \right) \right] \quad (13)$$

$P_{am}$ ,  $r$ ,  $z$ , and  $f^z$  were measured or calculated for each compound.  $A$  and  $B$  were determined by a multiple nonlinear regression using Eq. 14 (12).

$$Fa\% = 100 \times [1 - \exp(-A \times P_{tot})] \quad (14)$$

Fa% values were cited from the literature (3).

### Estimating the Contribution of Each Absorption Pathway

The contribution of each absorption pathway was estimated using the following equations:

$$P_{caco-2}^{para} = P_{caco-2}^{tot} - P_{am} \quad (15)$$

$$\%Para = \frac{P_{caco-2}^{para}}{P_{caco-2}^{tot}} \times 100 \quad (16)$$

$$\%Trans = 100 - \%Para \quad (17)$$

where  $P_{caco-2,tot}$  is the  $P_{app}$  in the Caco-2 monolayer,  $P_{caco-2,para}$  is the  $P_{app}$  of the paracellular pathway in the Caco-2 monolayer, %Para is the contribution of paracellular permeation, and %Trans is the contribution of transcellular permeation.

## RESULTS AND DISCUSSION

### Optimization of Pore Radius of TJs in Caco-2 Monolayers

$P_{app}$  values of 20 compounds, whose physicochemical properties differ, were measured in Caco-2 monolayers (Table I). Transepithelial electrical resistance (TEER) values were  $365 \pm 54 \Omega \cdot \text{cm}^2$  ( $n = 43$ ) in our Caco-2 monolayers and were appropriate values for performing the transport experiment. Large interexperimental variability was observed in some drugs (Table I). CV values in transport experiments were plotted against prologD values (Fig. 1A). Reproducibility among experiments tended to be low in hydrophilic drugs. To examine whether this variability is due to the variation in paracellular permeation, we used lucifer yellow (LY) as a paracellular marker compound, and the correlation between the  $P_{app}$  of hydrophilic drugs and that of LY was examined. A positive correlation was observed between the  $P_{app}$  of LY and that of hydrophilic drugs; for example, metformin and cefuroxime (Fig. 1B). Because paracellular permeation is greatly affected by pore radius of TJs, these results clearly indicated that the permeation of hydrophilic drugs across Caco-2 monolayers was influenced by the pore radius of TJs in each well; that is, the integrity of the monolayer. Therefore, in order to accurately measure  $P_{app}$  values, it is preferable to make corrections using the pore radius of TJs measured in each monolayer. The pore radius of TJs was calculated by Adson *et al.* (9). However, the method required the use of radioactive mannitol and urea as an internal standard for each well.

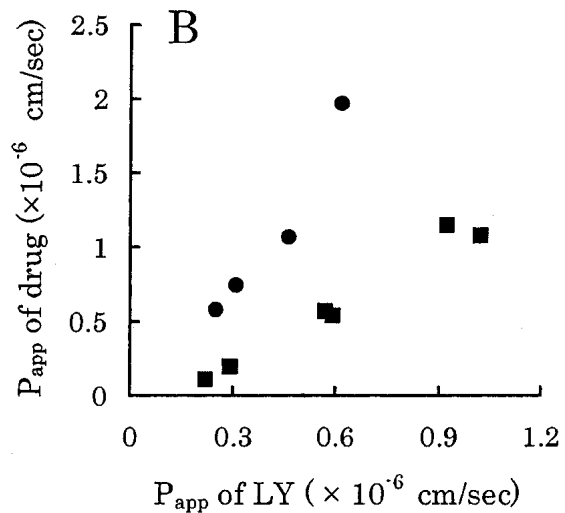
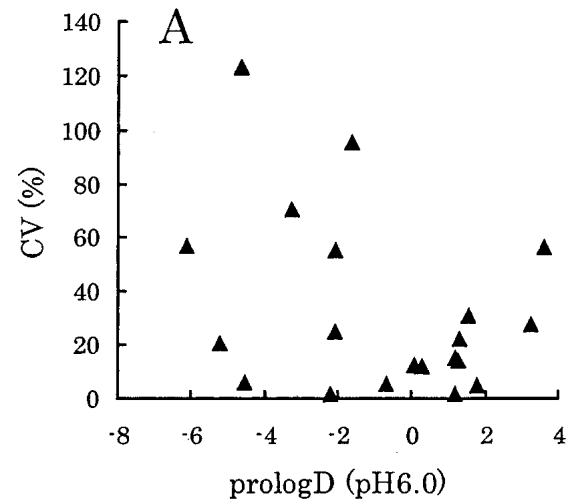


**Fig. 1.** (A) Relationship between lipophilicity of drugs and interexperimental variability in Caco-2 assay. (B) Correlation between  $P_{app}$  of Lucifer yellow (LY) and that of metformin (●) and cefuroxime (■) across Caco-2 monolayers.

Therefore, a more convenient method for calculating the pore radius of TJs from the  $P_{app}$  value of LY was examined. An excellent correlation was observed between the  $P_{app}$  of LY and the pore radius calculated by Adson's method (Fig. 2). So, pore radius can be estimated using Eq. 18:

$$R = 2.96 \times 10^6 \times P_{LY} + 4.94 \quad (18)$$

where  $R$  is the pore radius of TJs, and  $P_{LY}$  is the  $P_{app}$  of LY.

The optimum pore radius for predicting human Fa was determined as follows. As in Fig. 1B, the  $P_{app}$  measured in each monolayer was plotted against the pore radius of TJs, estimated from Eq. 18. A regression equation was obtained for each drug. Then, the  $P_{app}$  at three different pore radii for each drug was calculated from the regression equation and plotted against actual Fa in humans (Fig. 3). The fitting curve was obtained from the sigmoidal Eq. 19:

$$Fa\% = \frac{100 \times P_{caco-2}^a}{b^a + P_{caco-2}^a} \quad (19)$$

where  $a$  and  $b$  are coefficients.

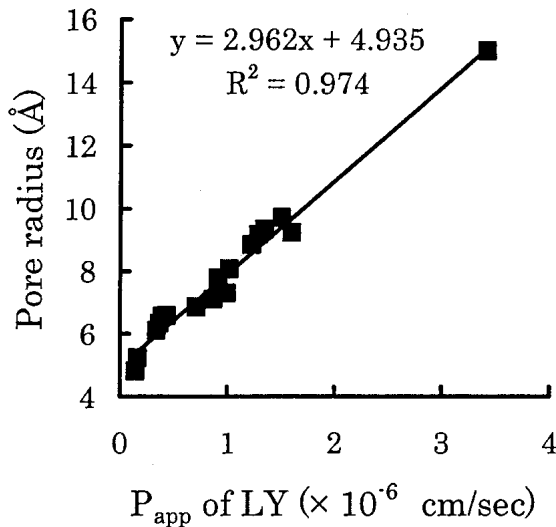


**Fig. 2.** Correlation between  $P_{app}$  of LY and pore radius of TJs in Caco-2 monolayers.

Analyzing the correlation between the actual and predicted Fa with various pore radii, the highest correlation coefficient was obtained at 7 Å (Fig. 3 and insert). These results indicate that the optimal pore radius of TJs for predicting Fa in humans is 7 Å in our Caco-2 monolayer. Therefore,  $P_{app}$  estimated in the current study was corrected using a pore radius of 7 Å. This value agreed well with the 6.7 Å to 7.9 Å pore radius of human jejunum reported by Fordtran (13) and Soerger (14).

**Prediction of Human Fa for a Hydrophilic Drug**

Although the Fa of many lipophilic drugs in humans exceeds 90%, values reported for hydrophilic drugs range from

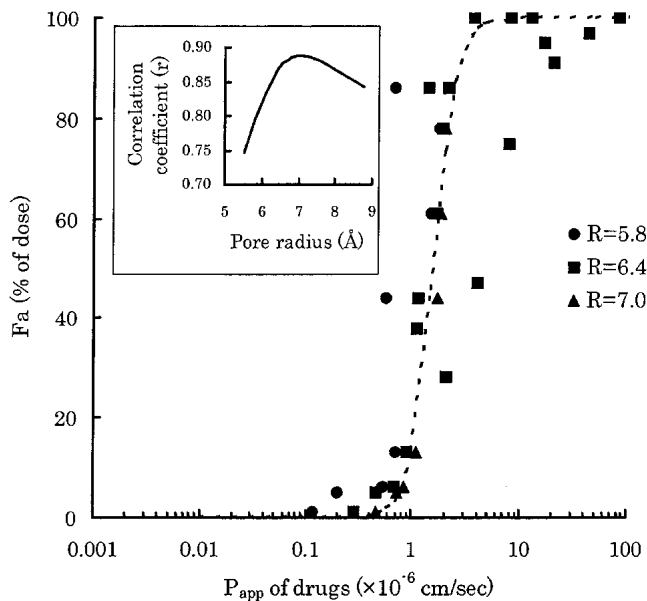


**Fig. 3.** Correlation between  $P_{app}$  across Caco-2 cell monolayers and fraction dose absorbed (Fa) in humans for the compounds listed in Table I at three different pore radii (R) of TJs. The dashed line was obtained by fitting the sigmoidal equation for the data of 7 Å. Insert: Correlation coefficient (r) at various pore radii was plotted. Optimal pore radius of TJs for predicting Fa in humans was set up with 7 Å in the Caco-2 cell model.

0% to 100% (15). In order to use drugs properly, information about Fa in humans is important. However, measurements cannot be performed easily because it is necessary to administer a radioactive compound. Therefore, to predict human Fa values of hydrophilic drugs based on data obtained *in vitro* will be helpful for setting an appropriate dosage. The correlation study between actual and predicted Fa values for the permeation of Caco-2 monolayers was examined using 10 hydrophilic drugs, the prologD of which was less than 0 at pH 6.0. A schematic diagram for predicting Fa in human is shown in Fig. 4. A large deviation from the unity line that is low predictability of Fa values was observed when the mean  $P_{app}$  was used (Fig. 5A). Because the slope of the correlation, around  $1 \times 10^{-6}$  cm/s, is quite steep, predicted Fa values are greatly affected by slight variations in  $P_{app}$  in this range (Fig. 3). The  $P_{app}$  of hydrophilic drugs varied with the size of the pore radius of TJs in Caco-2 monolayers, hence we examined whether the low predictability of Fa was caused by the variation in the pore radius of TJs in each experiment. The correlation between actual and predicted Fa values improved dramatically ( $r = 0.96$ ) using the  $P_{app}$  value corrected with the optimum pore radius of TJs (Fig. 5B). The result suggests that the low predictability of the Fa of hydrophilic drugs is due to the variation in pore radius and also indicates that the predictability was improved by the correction.

**Estimating the Contribution of Absorption Pathways**

The membrane permeation of a hydrophilic drug involves paracellular permeation, transcellular passive permeation, and carrier-mediated transport. It is important to comprehend the contribution of each pathway when analyzing the absorption mechanism of drugs. However, with the Caco-2 assay alone, it is difficult to measure  $P_{app}$  for the transcellular and paracellular routes, separately. Therefore, a comparison between Caco-2 assay and PAMPA, in which only transcellular permeability is measured, was examined.

The permeability of 20 compounds was assessed using both assays (Table I). Especially for a hydrophilic drug defined by a prologD less than 0 at pH 6.0 in this study, the correlation between the  $P_{app}$  obtained in the two assays was very low (Fig. 6A). The result may be explained by the lack of a paracellular pathway in PAMPA.

In order to correct the paracellular permeation of a hydrophilic drug in PAMPA, a PAMPA-PP-RF model has been advocated (3). The potential drop across the paracellular barrier ( $\Delta\psi$ ) in Caco-2 monolayers has been estimated to be 18

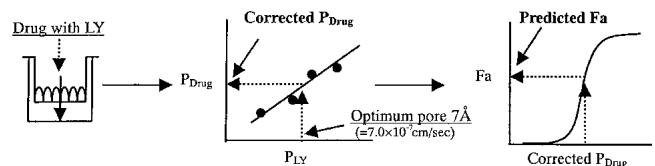


**Fig. 4.** Schematic diagram illustrating the prediction of Fa in human by Caco-2 monolayers.  $P_{app}$  of drug ( $P_{Drug}$ ) and LY ( $P_{LY}$ ) were measured in at least three independent experiments.  $P_{Drug}$  were plotted against  $P_{LY}$  in each well, and then regression equation was estimated. Corrected  $P_{Drug}$  at optimum pore radius of TJs (7 Å) was calculated using the regression equation. Finally, predicted Fa in human was estimated by substituting the corrected  $P_{Drug}$  in Fa prediction equation.

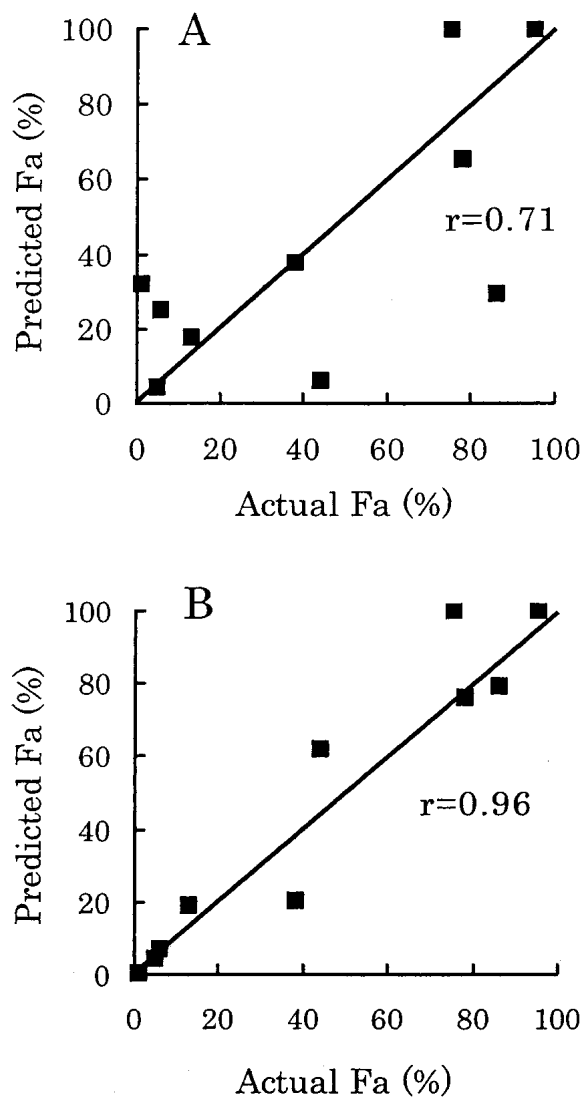


**Fig. 5.** Correlation between the reported and predicted fraction dose absorbed (Fa) of hydrophilic drugs in humans. The  $P_{app}$  of Caco-2 cell monolayers was corrected (A) before and (B) after using the pore radius of TJ ( $R = 7 \text{ \AA}$ ). The depicted line has a slope of unity.

mV (9). Thus, a pore radius of  $7 \text{ \AA}$  and  $\Delta\psi$  of 18 mV were used in this study. An improved correlation between the permeability of the Caco-2 monolayer and corrected permeability of PAMPA was observed for a hydrophilic drug (Fig. 6B). This result suggests that the paracellular pathway plays an important role in the permeation of hydrophilic drugs in Caco-2 monolayers. Zhu *et al.* reported a high correlation between the  $P_{app}$  obtained in the Caco-2 assay and that in the PAMPA even after correcting the latter value using the pore radius or  $\Delta\psi$  (16). The discrepancy would be due to the difference in the logD range of the drugs used [Zhu *et al.* (16):  $0.5 \pm 1.4$ , present;  $-0.8 \pm 2.8$ ].

Next, we tried to estimate the contribution of paracellular permeation to  $P_{app}$  in Caco-2 monolayers. Assuming that the passive transcellular permeation of a hydrophilic drug is equivalent to PAMPA and carrier-mediated transport of the drug is absent in Caco-2 monolayers, subtracting the  $P_{app}$  of PAMPA from that of Caco-2 can be considered to give the value of paracellular permeability. As shown in Table II, the

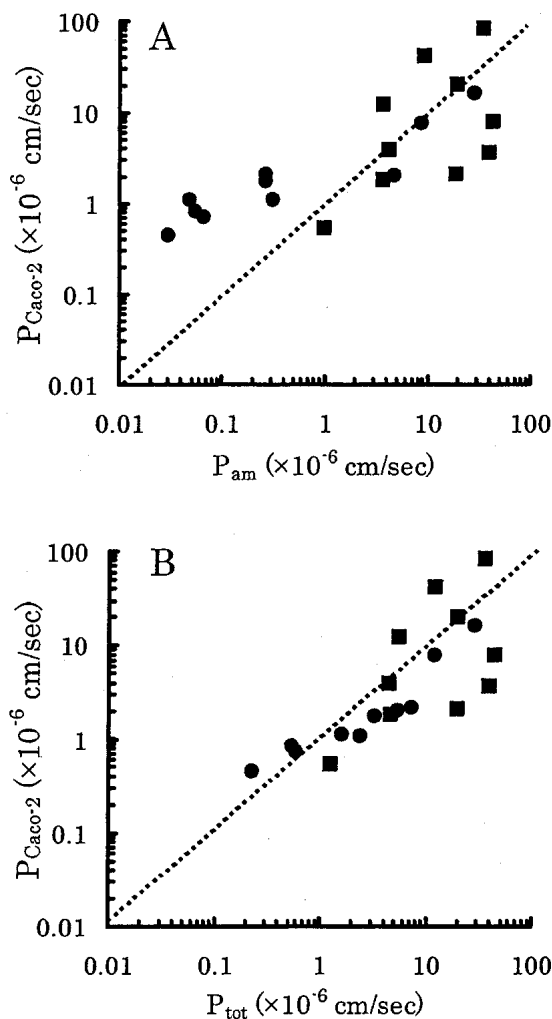


**Fig. 6.** Correlation between permeation of the artificial membrane and Caco-2 cell monolayer for tested compounds.  $P_{am}$  was corrected (A) before and (B) after using the Renkin function ( $R = 7 \text{ \AA}$  and  $\Delta\psi = 18 \text{ mV}$ ). Hydrophobic drug (prologD > 0) (■), hydrophilic drug (prologD < 0) (●). The dashed lines represent unity.

contribution of paracellular permeation was larger than that of transcellular permeation in many hydrophilic drugs *in vitro*. Though the Fa of metformin in humans was reported to be high, its contribution has not been discussed yet. In this

**Table II.** Relative Contribution of the Transcellular and Paracellular Pathways to the Transport of Hydrophilic Drugs Across Caco-2 Monolayers

Compound	Actual Fa%	Transcellular %	Paracellular %
Doxycycline	95	100	0
Metformin	86	12	88
Tetracycline	78	100	0
Guanabenz	75	100	0
Metaproterenol	44	15	85
Famotidine	38	4	96
Chlorothiazide	13	29	71
Cefazolin	6	7	93
Cefuroxime	5	9	91
Ceftriaxone	1	6	94

study, the  $P_{app}$  of metformin in PAMPA was quite low (Table I) and indicated a low permeation through the cell membrane. Also, the contribution of carrier-mediated transport is negligible for metformin absorption (17). Therefore, these observations suggest that metformin is absorbed mainly through the paracellular pathway in humans and may be an example where the contribution of paracellular permeation to drug absorption in humans is large.

## CONCLUSIONS

By correcting the pore radius of TJs in the Caco-2 monolayer, the reproducibility of  $P_{app}$  across Caco-2 cells and predictability of human Fa were much improved in hydrophilic drugs. Moreover, the contribution of each pathway to membrane permeation could be estimated by comparing the Caco-2 model and PAMPA. The new method is applicable to the following as well as drug development. The measurement of  $P_{app}$  in Caco-2 with or without concomitant drugs, which affects the pore radius of TJs, makes it possible to predict the change in human Fa caused by drug-drug interaction. Influence of interindividual variability of pore radius of TJs on human Fa may be predicted by the measurement of  $P_{app}$  at various physiological pore radii. And, the correction might solve the problem of p-glycoprotein assay in which the changes in *in vitro* monolayer integrity have an intense effect on substrate specificity and capacity of the transporter. Thus, the new method will contribute to evaluating the true effects of carrier-mediated transport as well as to setting appropriate dosages and to developing new drugs.

## REFERENCES

1. H. Bohets, P. Annaert, G. Mannens, L. V. Beijsterveldt, K. Anciaux, P. Verboven, W. Meuldermans, and K. Lavrijsen. Strategies for absorption screening in drug discovery and development. *Curr. Top. Med. Chem.* **5**:367–383 (2001).
2. P. Wils, A. Warnery, V. Phung-Ba, S. Legrain, and D. Scherman. High lipophilicity decreases drug transport across intestinal epithelial cells. *J. Pharmacol. Exp. Ther.* **269**:654–658 (1994).
3. K. Sugano, N. Takata, M. Machida, K. Saitoh, and K. Terada. Prediction of passive intestinal absorption using bio-mimetic artificial membrane permeation assay and the paracellular pathway model. *Int. J. Pharm.* **241**:241–251 (2002).
4. Y. L. He, S. Murby, G. Warhurst, L. Gifford, D. Walker, J. Ayton, R. Eastmond, and M. Rowland. Species differences in size discrimination in the paracellular pathway reflected by oral bioavailability of poly(ethylene glycol) and D-peptides. *J. Pharm. Sci.* **87**:626–633 (1998).
5. I. J. Hidalgo, T. J. Raub, and R. T. Borchardt. Characterization of the human colon carcinoma cell line (Caco-2) as a model system for intestinal epithelial permeability. *Gastroenterology* **96**:736–749 (1989).
6. P. Artursson, K. Palm, and K. Luthman. Caco-2 monolayers in experimental and theoretical predictions of drug transport. *Adv. Drug Deliv. Rev.* **46**:27–43 (2001).
7. S. Yamashita, T. Furubayashi, M. Kataoka, T. Sakane, H. Sezaki, and H. Tokuda. Optimized conditions for prediction of intestinal drug permeability using Caco-2 cells. *Eur. J. Pharm. Sci.* **3**:195–204 (2000).
8. G. T. Knipp, N. F. H. Ho, C. L. Barsuhn, and R. T. Borchardt. Paracellular diffusion in Caco-2 cell monolayers: effect of perturbation on the transport of hydrophilic compounds that vary in charge and size. *J. Pharm. Sci.* **86**:1105–1110 (1997).
9. A. Adson, T. J. Raub, P. S. Burton, C. L. Barsuhn, A. R. Hilgers, K. L. Audus, and N. F. H. Ho. Quantitative approaches to delineate paracellular diffusion in cultured epithelial cell monolayers. *J. Pharm. Sci.* **83**:1529–1536 (1994).
10. F. E. Curry. Handbook of physiology. In E. M. Renkin and C. C. Michel (eds.), *The Cardiovascular System*, American Physiology Society, Bethesda, MD, 1984, pp. 309–374.
11. K. Sugano, H. Hamada, M. Machida, H. Ushio, K. Saitoh, and K. Terada. Optimized conditions of bio-mimetic artificial membrane permeation assay. *Int. J. Pharm.* **228**:181–188 (2001).
12. G. L. Amidon, P. J. Sinko, and D. Fleisher. Estimating human oral fraction dose absorbed, a correlation using rat intestinal membrane permeability for passive and carrier-mediated compounds. *Pharm. Res.* **5**:651–654 (1988).
13. J. S. Fordtran, F. C. Rector, Jr., M. F. Ewton, and N. Soter. and J. Kinney. Permeability characteristics of the human small intestine. *J. Clin. Invest.* **44**:1935–1944 (1965).
14. K. H. Soergel, G. E. Whalen, and J. A. Harris. Passive movement of water and sodium across the human small intestinal mucosa. *J. Appl. Physiol.* **24**:40–48 (1968).
15. M. E. Dowty and C. R. Dietsch. Improved prediction of *in vivo* peroral absorption from *in vitro* intestinal permeability using an internal standard to control for intra- and inter-rat variability. *Pharm. Res.* **14**:1792–1797 (1997).
16. C. Zhu, L. Jiang, T. M. Chen, and K. K. Hwang. A comparative study of artificial membrane permeability assay for high throughput profiling of drug absorption potential. *Eur. J. Med. Chem.* **37**:399–407 (2002).
17. N. C. Sambol, L. G. Brookers, J. Chiang, A. M. Goodman, E. T. Lin, C. Y. Liu, and L. Z. Benet. Food intake and dosage level, but not tablet vs solution dosage form, affect the absorption of metformin HCl in man. *Br. J. Clin. Pharmacol.* **42**:510–512 (1996).
18. K. Seiga, M. Minakawa, K. Miyoshi, K. Yamaji, and Y. Sugiyama. Studies on cefazolin. 2. Primary clinical trial by oral administration. *Jpn. J. Antibiot.* **25**:28–30 (1972).
19. E. S. Rattie and L. J. Ravin. Pharmacokinetic interpretation of blood levels and urinary excretion data for cefazolin and cephalothin after intravenous and intramuscular administration in humans. *Antimicrob. Agents Chemother.* **7**:606–613 (1975).